On the calculation of the Kalker's creep coefficients for non-elliptical contact areas

J. Gómez-Bosch*, J. Giner-Navarro* and J. Carballeira*

*Instituto Universitario de Ingeniería Mecánica y Biomecánica
Universitat Politècnica de València
Valencia, Spain
e-mail: jorgobos@upvnet.upv.es, juanginer@upv.es and jacarmo@mcm.upv.es

Key words: Contact Mechanics, Railway Dynamics, Tangential Contact Problem, FastSim, Non-Hertzian Contact

Abstract: *FastSim is the most widely used tangential contact method due to its accuracy and computational efficiency. However, its use is limited to elliptic contact areas, as it needs results from Kalker's Linear Theory, a Hertzian contact theory, to obtain the so-called elastic parameters. This makes FastSim unable to face some of the current railway challenges, such as wear, corrugation, Rolling Contact Fatigue (RCF), wheel flats, etc. Taking this limitation into account, in the present work, an alternative methodology to Kalker's Linear Theory is proposed, which will enable FastSim to deal with non-Hertzian conditions.*

1 INTRODUCTION

Solving the tangential wheel-rail contact problem is always complex. Depending on the application, a trade-off between accuracy and computational cost is required. The most accurate tangential contact model existing is CONTACT [1, 2], but, because of its high computational cost, it is mainly used as a reference theory for validation. In railway dynamics simulation, simplified contact theories [3, 4, 5, 6] are usually required. These theories are much more computationally efficient, although they are less accurate. Among all the simplified theories, the most widely used is FastSim [6], due to its high-level performance and accuracy, and its ability to predict tangential stresses distribution and the stick-slip boundary [7]. FastSim is a contact theory that assumes that the surface displacements on a point are only related to the tangential stress on that point through the so-called elastic parameters [8]. To obtain these parameters, creep forces resulting from the full adhesion solution [8] (simplified contact theory which assumes adhesion over the entire contact area) are equalled to the ones obtained through Kalker's Linear Theory (KLT) [9] (exact contact theory but limited to Hertzian contact conditions). It is this limitation which has led various authors to find alternative methods to obtain these elastic parameters under non-Hertzian contact conditions [8, 10, 11], and so, to be able to extend FastSim validity to non-elliptic contact areas. The elastic parameter calculation under non-Hertzian condition has been carried out according to two different approaches [11]: a first approach, based on associating the contact area to one or several equivalent ellipses [12, 13]; and a second approach, in which, for each particular contact geometry, elastic parameters are obtained by solving the exact contact problem [8, 10]. Despite the methods based on the second approach are quite more accurate, their computational cost is much higher than the ones based on the first approach. That is the reason why equivalent ellipse based methods are used nowadays to study the influence of the non-Hertzian contact in actual railway vehicle dynamics [14, 15], as well as in complex tangential contact phenomena, such as wear [16, 17], Rolling Contact Fatigue (RCF) [18], wheel out-of-roundness [19, 20], etc.

In the present work, an alternative tangential contact model to KLT which allows the elastic parameters calculation under non-Hertzian hypothesis is proposed. This model derives from Kalker's Variational Theory [8], to which steady-state and full adhesion hypothesis are imposed.

https://doi.org/10.4995/YIC2021.2021.12313

Since the exact contact is solved to obtain the elastic parameters using this model, it is included within the second approach described above. Nevertheless, this model presents some advantages compared to existing alternatives [8, 10], as its resolution is not iterative, nor stress solutions are approximated to any polynomic function. These advantages make this model more suitable to face the new railway challenges, as the ones listed above.

The mathematical model of this work is developed in Section 2. In Section 3, the accuracy of the proposed contact model is analysed, when results are compared to the ones obtained with KLT on elliptic contact areas. Finally, in Section 4, according to presented results, the contribution of this work is concluded and justified.

2 MATHEMATICAL MODEL

In the present work, a mobile reference frame $\mathbf{X}_1\mathbf{X}_2\mathbf{X}_3$ is assumed, with origin at the theoretical contact point, and it moves with it as the vehicle travels along the track. $\mathbf{X}_1$ axis is parallel to the rolling direction, $\mathbf{X}_3$ axis is normal to the contact, being positive to the wheel, and $\mathbf{X}_2$ axis corresponds to the lateral direction in order to form a right-handed rectangular frame, as it is shown in Figure 1.

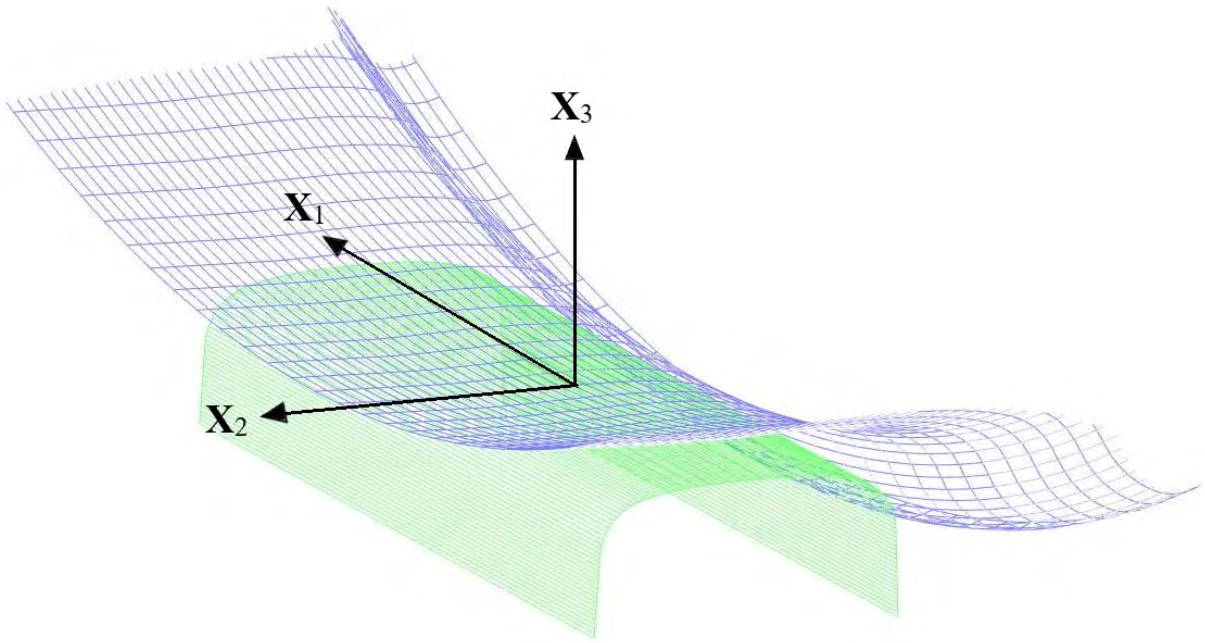

Figure 1: Mobile reference frame $\mathbf{X}_1\mathbf{X}_2\mathbf{X}_3$ at the theoretical contact point between rail (green) and wheel (blue).

As it is done in Kalker's Variational Theory [8], the kinematic equation that relates the rigid body displacements of the bodies in contact with the slip velocities and the elastic deformations can be written

$$\mathbf{s} = \mathbf{w} + 2\frac{D\mathbf{u}}{Dt} = \mathbf{w} + 2\frac{\partial \mathbf{u}}{\partial t} + 2V\frac{\partial \mathbf{u}}{\partial x_1}, \tag{1}$$

where $\mathbf{s}$ are the local slip velocities, $\mathbf{u}$ are the displacements related to the elastic deformation of the bodies in contact, V is the vehicle speed, and $\mathbf{w}$ are the velocities associated to the

undeformed configuration, which can be calculated from the creepages [8]. Assuming the steady-state hypothesis $\left(\frac{\partial}{\partial t}=0\right)$ and the full adhesion hypothesis ($\mathbf{s}=0$), Eq. (1) re-writes

$$\mathbf{w}=-2V\frac{\partial \mathbf{u}}{\partial x_1}. \tag{2}$$

Including the constitutive relationships in Eq. (2), it is possible to obtain an expression, which provides tangential stresses under steady-state and full adhesion conditions $\bar{p}_\tau$:

$$\mathbf{w}=-2V\left(\int_S \frac{\partial \mathbf{c}_1(\mathbf{x},\mathbf{y})}{\partial x_1}\bar{p}_1(\mathbf{y})+\frac{\partial \mathbf{c}_2(\mathbf{x},\mathbf{y})}{\partial x_1}\bar{p}_2(\mathbf{y})\right)ds(\mathbf{y}), \tag{3}$$

where $\mathbf{c}_1(\mathbf{x},\mathbf{y})$ and $\mathbf{c}_2(\mathbf{x},\mathbf{y})$ are two vectors that contain the elastic influence functions, and S is the contact surface. To solve Eq. (3), the contact area is discretised analogously as it is done in the TANG algorithm [8], assuming constant stresses on each element. For the j-th element of the mesh, Eq. (3) writes

$$\mathbf{w}^j=-2V\mathbf{C}^j\bar{\mathbf{p}}, \tag{4}$$

where $\mathbf{C}^j$ is the vector which contains the elastic influence coefficients derivatives, and $\bar{\mathbf{p}}$ is the column vector which contains tangential stresses under adhesion conditions of every element of the mesh. Figure 1 shows a scheme of the mesh used for solving Eq. (4), where a and b are half the size of the element on longitudinal and lateral directions, respectively. This equation is solved by a collocation method [1, 21], where the location of the collocation point can be controlled with a parameter α, which takes values in the range $[-1,1]$.

Once the tangential stresses have been obtained, the tangential contact forces can be obtained by summation of these stresses. As it is assumed that every element on the contact area is under adhesion, the tangential stresses and forces will be linear with creepages. By analogy with KLT, tangential forces under adhesion conditions $\bar{F}_\tau$ can be written as

$$\bar{F}_1=-f_{11}^*\xi \tag{5}$$

$$\bar{F}_2=-f_{22}^*\eta-\ f_{23}^*\phi, \tag{6}$$

where f_{11}^*, f_{22}^* and f_{23}^* are the analogous coefficients to the creep coefficients f_{11}, f_{22} and f_{23} defined by Kalker in Ref. [9]; and ξ, η and ϕ are longitudinal, lateral and spin creepages, respectively.

3 RESULTS

Using KLT creepage coefficients as a reference, it is possible to study the influence of the collocation point and the number of elements N on the accuracy of the results provided by the proposed method, for different ellipse axes ratio, r. Figure 2 shows the ratio between the creepage coefficients obtained by the proposed method and the ones obtained from KLT as a function of the location of the collocation point, for a mesh size of $N=6400$. Results for coefficients f_{11}^* and f_{22}^* are quite similar: the optimum collocation point is located at the centre of the element. Instead, to achieve higher accuracy on the f_{23}^* coefficient, it is convenient to move the collocation point forward to a value of parameter $\alpha=0.5$.

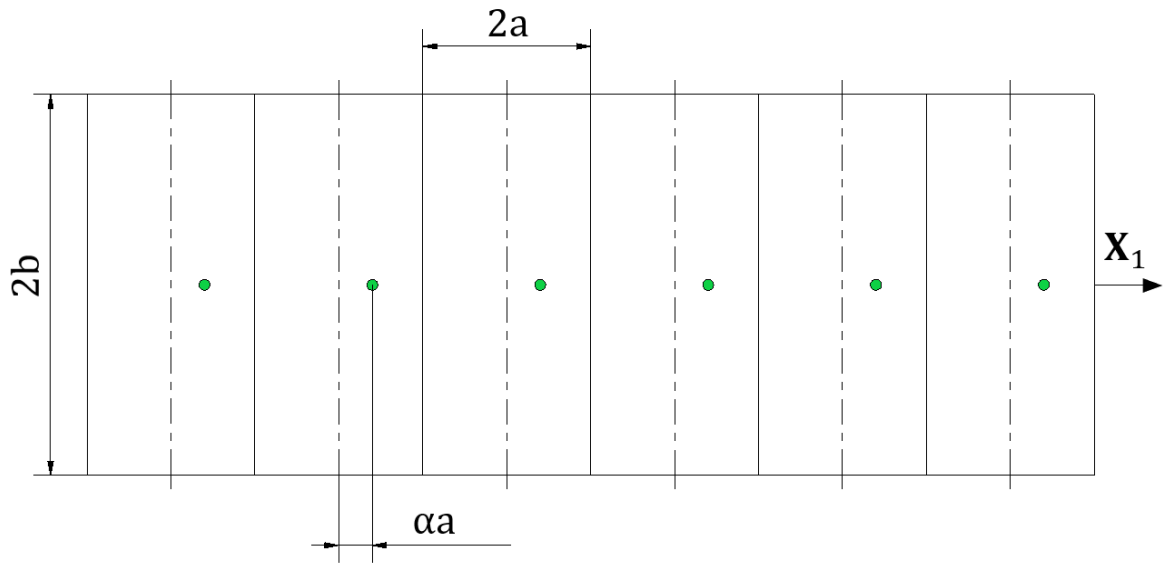

Figure 2: Mesh scheme with collocation points (green dots).

Figure 3 shows the evolution of the creepage coefficients ratio as a function of the number of elements of the mesh, N, for a collocation point at the centre of the element. According to these results, despite the ratio is close to 1 for a sufficient number of elements, thus being the error acceptable, the method does not present convergence. Assuming the full adhesion hypothesis leads to infinite tangential stress at the trailing edge of the contact area, which produces numerical errors, and the non-convergence of the method, as it is also concluded in Ref. [22].

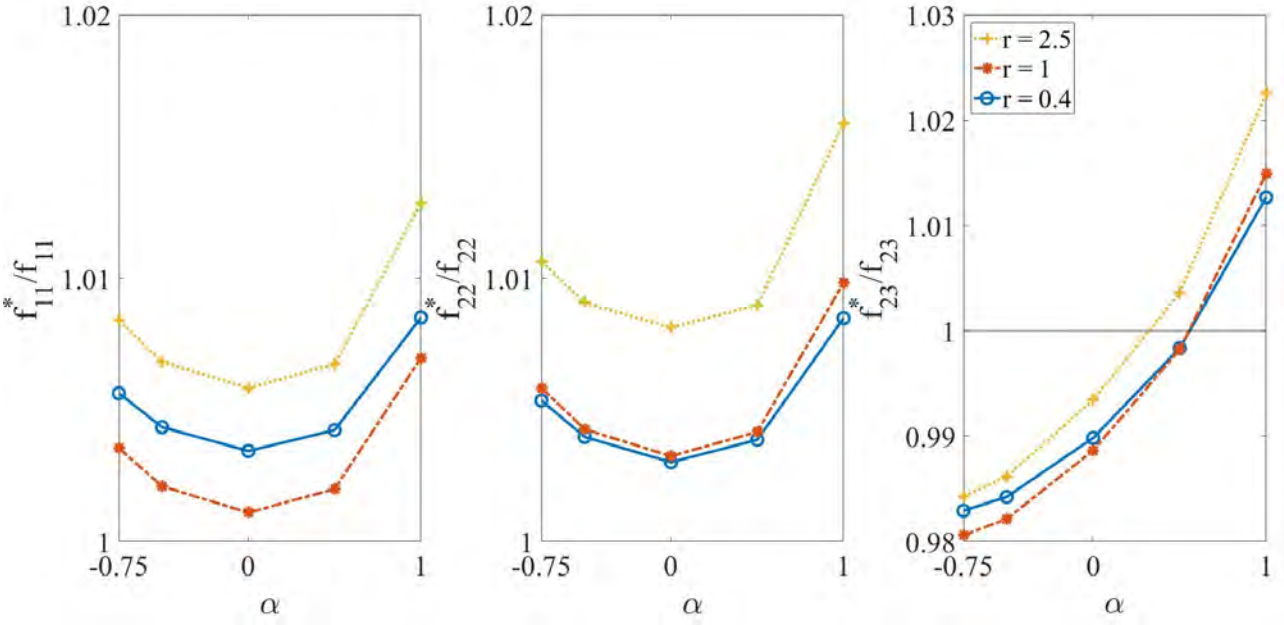

Figure 3: Creep coefficients ratio as a function of the collocation parameter α for three different ellipse ratios r. The number of elements of the mesh is $N = 6400$.

As coefficients f_{11}^* and f_{22}^* are the most relevant for tangential forces calculation, optimum collocation point is located at the centre of the element. The optimum mesh size is conditioned by the computational cost. To solve Eq. (4), it is needed to invert a $2N \times 2N$ matrix, so that, increasing the mesh size, exponentially increases the calculation time. Increasing mesh size from $N = 60 \times 60$ to$N = 80 \times 80$ elements implies four times more calculation time, but only a reduction of creep coefficients absolute error calculation of 0.2%. Therefore, as $N = 60 \times 60$ is the smallest mesh size with absolute errors on f_{11}^* and f_{22}^* calculations below 1%, authors propose an optimum mesh size of $N = 60 \times 60$ elements.

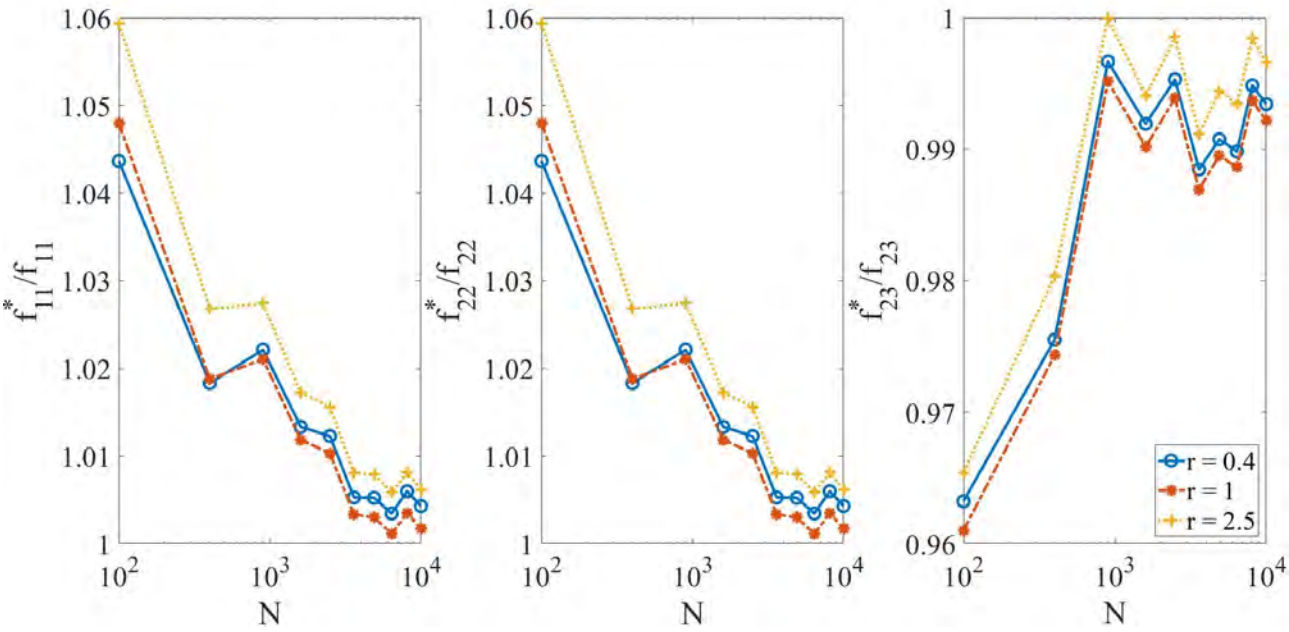

Figure 4: Creepage coefficients ratio as a function of the number of elements of the mesh N for three different ellipse ratios r. The collocation point is located at the centre of the element.

4 CONCLUSION

The FastSim algorithm is limited to elliptical contact areas because of the calculation of the elastic parameters based on Kalker's Linear Theory results. In this work, an alternative model has been proposed to deal with that restriction, allowing the calculation of the creep coefficients for non-Hertzian contact conditions, which can be used to obtain the elastic parameters according to the FastSim methodology. Based on results shown in this work, it has been proved that, combining both optimum collocation point ($\alpha = 0$) and mesh size ($N = 60 \times 60$ elements), sufficient to minimize the numerical error associated with the full adhesion hypothesis assumption, without considerably increasing the computational calculation time, the present model gives fairly accurate results on creep coefficients calculation for elliptic contact areas, without assuming Hertzian contact hypothesis. So, on future research, this method will be used together with FastSim to obtain results on tangential forces and stress distributions on non-Hertzian contact conditions.

AKNOWLEDGEMENTS

The authors gratefully acknowledge the financial support of Agencia Estatal de Investigación and European Regional Development Fund (grant PRE2018-084067 and project TRA2017-84701-R).

REFERENCES

[1] J. J. Kalker, "The computation of three-dimensional rolling contact with dry friction," International Journal for Numerical Methods in Engineering, vol. 14, no. 9, pp. 1293-1307, 1979.

[2] J. J. Kalker, Users Manual of the Fortran Program CONTACT, Delft: Delft University of Technology, Departament of Math. and Computer Science, 1986.

[3] K. L. Johnson, "The effect of spin upon the rolling motion of an elastic sphere on a plane," Journal of Applied Mechanics, vol. 25, pp. 332-338, 1958.

[4] P. J. Vermeulen and K. L. Johnson, "Contact of Nonspherical Elastic Bodies Transmitting Tangential Forces," Journal of Applied Mechanics, vol. 31, no. 2, pp. 338-340, 1964.

[5] O. Polach, "A Fast Wheel-Rail Forces Calculation Computer Code," Vehicle System Dynamics, vol. 33, no. 1, pp. 728-739, 1999.

[6] J. J. Kalker, "A fast algorithm for the simplified theory of rolling contact," Vehicle System Dynamics, vol. 11, no. 1, pp. 1-13, 1982.

[7] M. S. Sichani, R. Enblom and M. Berg, "An alternative to FASTSIM for tangential solution of the wheel-rail contact," Vehicle System Dynamics, vol. 54, no. 6, pp. 748 - 764, 2016.

[8] J. J. Kalker and K. L. Johnson, Three-Dimensional Elastic Bodies in Rolling Contact, Delft: ASME. J. Appl. Mech., 1993.

[9] J. J. Kalker, On the rolling contact of two elastic bodies in the presence of dry friction, T. H. Delft: Thesis, 1967.

[10] K. Knothe and L. T. Hung, "A method for the analysis of the tangential stresses and the wear distribution between two elastic bodies of revolution in rolling contact," Solids Structures, vol. 21, no. 8, pp. 889-906, 1985.

[11] M. S. Sichani, R. Enblom and M. Berg, "Comparison of non-elliptic contact models: Towards fast and accurate modelling of wheel-rail contact," Wear, vol. 314, no. Issues 1-2, pp. 111-117, 2014.

[12] J. Piotrowski and W. Kik, "A simplified model of wheel/rail contact mechanics for non-Hertzian problems and its application in rail vehicle dynamic simulations," Vehicle System Dynamics, vol. 46, no. 1-2, pp. 27-48, 2008.

[13] J. B. Ayasse and H. Chollet, "Determination of the wheel rail contact patch in semi-Hertzian conditions," Vehicle System Dynamics, vol. 43, no. 3, pp. 161-172, 2005.

[14] B. Liu and S. Bruni, "Comparison of wheel-rail contact models in the context of multibody system simulation: Hertzian versus non-Hertzian," Vehicle System Dynamics, pp. 1 - 21, 2020.

[15] Q. Guan, B. Liu and S. Bruni, "Effects of Non-Hertzian Contact Models on Derailment Simulation," in Proceedings of the 2020 Joint Rail Conference. 2020 Joint Rail Conference., St. Louis, Missouri, USA, 2020.

[16] G. Tao, Z. Wen, X. Zhao and X. Jin, "Effects of wheel-rail contact modelling on wheel wear simulation," Wear, Vols. 366 - 367, pp. 146 - 156, 2016.

[17] M. Meacci, Z. Shi, E. Butini, L. Marini, E. Meli and A. Rindi, "A railway local degraded adhesion model including variable friction, energy dissipation and adhesion recovery," Vehicle System Dynamics, pp. 1 - 22, 2020.

[18] S. Hossein-Nia, M. S. Sichani, S. Stichel and C. Casanueva, "Wheel life prediction model - an alternative to the FASTSIM algorithm for RCF," Vehicle System Dynamics, vol. 56, no. 7, pp. 1051 - 1071, 2018.

[19] G. Tao, Z. Wen, G. Chen, Y. Luo and X. Jin, "Locomotive wheel polygonisation due to discrete irregularities: simulation and mechanism," Vehicle System Dynamics, vol. 59, no. 6, pp. 872 - 889, 2021.

[20] U. Spangenberg, "Variable frequency drive harmonics and interharmonics exciting axle torsional vibration resulting in railway wheel polygonisation," Vehicle System Dynamics, vol. 58, no. 3, pp. 404 - 424, 2020.

[21] J. G. Giménez, A. Alonso and L. Baeza, "Precision analysis and dynamic stability in the numerical solution of the two-dimensional wheel/rail tangential contact problem," Vehicle System Dynamics, vol. 57, no. Issue 12, pp. 1822-1846, 2019.

[22] A. Alonso and J. G. Giménez, "Tangential problem solution for non-elliptical contact areas with the FastSim algorithm," Vehicle System Dynamics, vol. 45, no. 4, pp. 341-357, 2007.